POLISH MARITIME RESEARCH 3 (123) 2024 Vol. 31; pp. 25-33
10.2478/pomr-2024-0033

Numerical Investigation of the Effects of Aspect Ratio on the Hydrodynamic Performance of a Semi-Planing Catamaran

AliAsghar Moghaddas
Amirkabir University of Technology, Department of Maritime Engineering, Tehran, Islamic Republic of Iran
Hamid Zeraatgar*
Amirkabir University of Technology, Tehran, Islamic Republic of Iran

* Corresponding author: *hamidz@aut.ac.ir (Hamid Zeraatgar)*

ABSTRACT

A semi-planing catamaran is a type of marine craft that benefits from high speed, in conjunction with the its inherent characteristics such as a large deck and high transverse stability. The aspect ratio, length over the beam of a demi-hull, significantly affects the hydrodynamic performance of this vessel. In this study, the effects of the aspect ratio on the hydrodynamic performance of a semi-planing catamaran in calm water and waves are investigated using numerical simulations. The numerical simulation of the AUT-SEM00 model itself is validated by its model test results. The results show that increasing the aspect ratio significantly increases the wetted surface, and that the increase in resistance in calm water is negligible. In addition, increasing the aspect ratio radically reduces the amplitude of vertical acceleration in waves at the center of gravity by up to 85%. Consequently, the seakeeping performance is considerably improved, and the risk to crew and equipment is reduced.

Keywords: semi-planing catamaran, aspect ratio, CFD, calm water, waves

Catamarans have a wide range of applications as small sailing boats, medium-sized passenger ships, and large naval vessels. They can be categorised as displacement vessels, semi-planing, or planing craft. Despite the variety in the types of catamaran, they have two main features in common: a large deck, and high transverse stability. The hydrodynamics of the ship can be evaluated based on several performance functions, such as resistance, propeller efficiency, seakeeping (low acceleration as a main feature), maneuverability, and so on. The most important forms of hydrodynamic performance for semi-planing and planing vessels are generally resistance and seakeeping. A new concept for a semi-planing hull may enable improvements in the resistance and/or seakeeping, and one of the geometric parameters that can improve the hydrodynamic performance of the catamaran is the aspect ratio, which for a conventional semi-planing catamaran is about 10. Semi-planing high-aspect-ratio twin-hull (HARTH)-type catamarans may have a much larger aspect ratio of 30, and the distance between the demi-hulls may also be larger than for conventional catamarans. The effects of aspect ratio on the performance of a HARTH-type semi-planing catamaran in calm water and waves form the main focus of this study.

Many research studies have been conducted on the subject of catamarans. Millward [1] analyzed the effect of the interference factor (IF) and water depth on catamaran resistance using an analytical method, and found that as the distance between demi-hulls decreased, the resistance

gradually increased. Zaraphonitis et al. [2] conducted both experimental and numerical studies on three Wiggly-shaped catamarans at Froude numbers (Fr) of 0.25–0.55 and IF values of 0.2–0.4. They concluded that the largest resistance corresponded to the smallest IF. Moraes et al. [3] conducted an analytical study of wave-making resistance for high-speed catamarans with U- and V-shaped sections at values of Fr of 0.2–0.9 and IF of 0.2–1.0. They found that the use of U or V-shaped sections did not affect the resistance for an IF larger than 0.6, and that the effect of IF on the wave-making resistance was insignificant. Lee et al. [4] studied a small catamaran at values of Fr of 0.2–0.9 and IF of 0.12–0.39 using both experimental and numerical methods. The results showed that decreasing the IF increased the trim and sinkage of the catamaran. Zaghi et al. [5,6] conducted experimental and numerical studies on the effects of IF on high-speed catamarans at Fr numbers of 0.2–0.8 and an IF of 0.17–0.3. The results showed that reducing the distance between two demi-hulls increased the trim angle, meaning that the centre of pressure moved forward and increased the sinkage of the catamaran. Farkas et al. [7] conducted a numerical study of the interaction of the resistance components for a 60-series catamaran at Fr numbers of 0.3–0.55 and an IF 0.23–0.47. They concluded that for high Fr, the generated waves were of a divergent type, while they were of a transverse type at moderate Fr, and that the interference of the transverse waves caused the formation of a wave trough in the stern, thereby increasing the resistance, trim and sinkage. Lin et al. [8] investigated the seakeeping performance of a wave-piercing catamaran called CAT-I using a numerical method based on Star CCM+ software, a RANS method and a potential flow method. Their results indicated that of these three methods, the RANS results coincided best with the experimental results. Fitriadhy et al. [9] conducted a numerical study of a V-shaped high-speed catamaran at Fr numbers of 0.5 and 1.0, and reported that the heave and pitch response amplitude operator (RAO) decreased as the wavelength increased for wavelengths less than 0.75 m. As the wave height increased, the heave and pitch RAO increased. Chen et al. [10] investigated a high-order boundary element method (HOBEN) for the evaluation of the performance of a high-speed catamaran at Fr numbers of 0.1–1.0 and an IF of 0.2–1.0. The results showed that for Fr > 0.5, the waves generated between the two demi-hulls were of the divergent type, and that the interaction caused by transverse waves was negligible. Honaryar et al. [11] investigated the dynamic response of a catamaran and showed that not only was its resistance substantially reduced by up to 15%, but also that the trim angle was diminished by 30% as the IF was decreased in the semi-planing and planing modes. Dogrul et al. [12] focused on a numerical investigation of a Delft 372 catamaran, which is widely used as a benchmark. Unsteady RANS analyses were conducted at Fr = 0.3 in regular head waves, and it was concluded that the effects of IF in waves were highly important for catamarans. Farkas et al. [13] numerically studied the effect of interference for a Delft 372 catamaran; the results for the wave profile revealed that at a lower value of Fr, a larger wave crest was obtained behind the stern of the ship compared to the wave crest at a higher Fr. Windyandari et al. [14] numerically investigated a hexagonal form for a catamaran hull in terms of the variation in deadrise angle, angle of attack, and stern angle. Their results showed that hexagonal catamaran hulls yielded better seakeeping performance in the beam sea. However, a conventional catamaran was found to be superior over a hexagonal catamaran under bow quartering and head sea conditions [14].

Although the aspect ratio has been shown to have a crucial effect on the performance of a catamaran, the references cited above indicate that its effects on the performance of a semi-planing catamaran (SPC) have not been addressed. The novelty of this study lies in the fact that we investigate the hydrodynamic performance of an SPC in calm water and waves under extreme changes in its aspect ratio. For this purpose, we first consider a conventional SPC denoted as AUT-SEM00, with a typical aspect ratio. Our numerical setup is validated using model test results for AUT-SEM00 [15], and is then employed to simulate two new SPC hulls, denoted as AUT-SEM01 and AUT-SEM02, which have aspect ratios of 19.18 and 29.61, respectively. Finally, the results for these three hull forms under calm water and waves are analyzed and compared to each other, and improvements are identified.

The main goal of this study is to improve the seakeeping of this type of vessel while keeping the resistance almost unchanged. Parameters such as rise-up (sinkage), dynamic trim, wetted surface, etc. are not regarded as indicators of the vessel's performance; instead, they are a kind of intermediate parameter. Of course, these parameters should not impose any undesirable behavior on the vessel.

CFD SET-UP VERIFICATION AND VALIDATION

GOVERNING EQUATIONS

The governing equations are the conservation of mass and Navier–Stokes equations in three dimensions, which can be expressed in the form of the RANS equations. The flow is assumed to be incompressible. The RANS equations are given in Eqs. (1) and (2):

$$\frac{\partial(\rho\overline{u_i})}{\partial t}+\frac{\partial}{\partial x_j}\left(\rho\overline{u_i}\,\overline{u_j}+\rho\overline{u_i'u_j'}\right)=\frac{\partial\bar{p}}{\partial x_i}+\mu\frac{\partial}{\partial x_j}\left(\frac{\partial\overline{u_j}}{\partial x_i}+\frac{\partial\overline{u_i}}{\partial x_j}\right) \quad (1)$$

$$\frac{\partial(\rho\overline{u}_i)}{\partial x_i}=0 \quad (2)$$

SHIP MODEL SPECIFICATIONS

The benchmark model on which the numerical settings and towing tank model tests were performed is denoted as AUT-SEM00. The specifications of AUT-SEM00 as an SPC at the full scale and the model scale are given in Table 1.

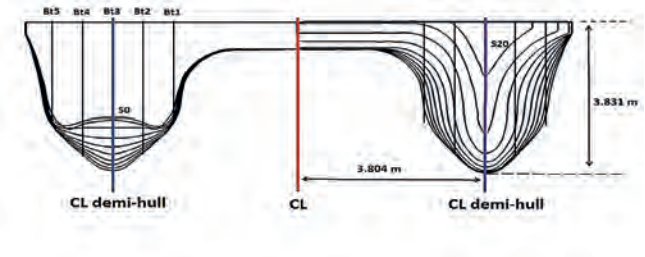

Fig 1. The body plan of AUT-SEM00

Tab. 1. Specifications of the AUT-SEM00 ship and model

Parameter	Symbol	Unit	Ship	Model
Overall length	L_{OA}	m	37.50	2.250
Waterline between perpendiculars	L_{PP}	m	34.73	2.083
Total breadth	B_T	m	11.21	0.672
Draught	T	m	1.81	0.109
Displacement	Δ	kg	161570	34.12
Water density	ρ	kg/m³	1025	1002
Scale	λ	–	1:1	1:16.67
Service speed	V	kn or m/s	30.0 (kn)	3.78 (m/s)
Longitudinal centre of gravity	L_{CG}	m	14.06	0.844
Static trim angle	θ_S	deg	2.00	2.00

CFD SETUP

Numerical simulations were conducted using Star CCM+ software, based on the ITTC recommendations of 2011 [16]. According to these recommendations, the distance between the flow inlet and the model should be between 1L and 2L, and the distance between the model and the flow outlet should be between 3L and 5L. In this case, the vertical distance between the model and the bottom of the domain is 2L, and the vertical distance between the model and the top of the domain is 3L. The dimensions of the domain were chosen according to the ITTC recommendations, and were appropriate for the dimensions of the NIMALA towing tank. A half model and related domain and mesh are shown in Fig. 2, and were dopted for simulations where the model and domain were symmetric. The two-equation model was chosen to solve the Reynolds stress equation.

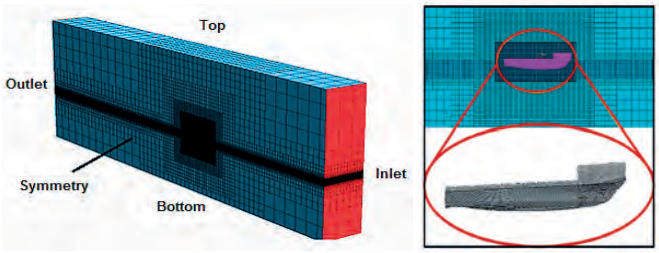

Fig 2. CFD simulation domain and mesh distribution

GRID VERIFICATION (GCI METHOD)

The grid convergence index (GCI) was applied to investigate the effects of the number of grids on the simulation results. The GCI method developed by Celik et al., which is widely employed, was used for investigation [17]. This method is given in Eqs. (3) to (9).

$$p = \frac{1}{ln(r_{21})}\left|ln\left|\varepsilon_{32}/\varepsilon_{21}\right| + q(p)\right| \tag{3}$$

$$q(p) = ln\left(\frac{r_{21}^{p} - s}{r_{32}^{p} - s}\right) \tag{4}$$

$$s = 1.sgn\left(\varepsilon_{32}/\varepsilon_{21}\right) \tag{5}$$

$$\varphi_{ext}^{21} = \frac{\left(r_{21}{}^{p}\varphi_1 - \varphi_{2)}\right)}{\left(r_{21}{}^{p} - 1\right)} \tag{6}$$

$$e_a^{21} = \left|\frac{\varphi_1 - \varphi_2}{\varphi_1}\right| \tag{7}$$

$$e_{ext}^{21} = \left|\frac{\varphi_{ext}^{21} - \varphi_1}{\varphi_{ext}^{21}}\right| \tag{8}$$

$$GCI_{fine}^{21} = \frac{1.25e_a^{21}}{r_{21}^{p} - 1} \tag{9}$$

Tab. 2. GCI parameters

Number of grids	N_1	**1263692**
	N_2	**866150**
	N_3	**625630**
r_{21}		1.21
r_{32}		1.17
$Ø_1$		32.18
$Ø_2$		32.80
$Ø_3$		36.92
$Ø^{21}_{ext}$		32.11
e^{21}_{a}		0.019
e^{21}_{ext}		0.0022
GCI^{21}_{fine}		0.00278

From Table 2, we see that the GCI method gives an error of 0.28% in the case of a fine mesh of 1.2 million grids. A further increase in the number of grids results in a very small improvement of less than 0.28%, and this is therefore regarded as an adequate number of grids.

VALIDATION OF CFD SIMULATION RESULTS

Moghaddas and Zeraatgar conducted a set of model tests in calm water and waves in a NIMALA towing tank [15]. Resistance tests were performed at a static trim angle of 2° over a full range of speeds. Model tests in waves were conducted at a speed of 3.78 m/s, a value equivalent to 30 knots for a ship. The tests in waves were conducted under head conditions for three regular waves with pitch and acceleration at the centre of gravity. The scheme in Fig. 3 illustrates the model, connections, and measurement locations, while Fig. 4 shows a photograph of the AUT-SEM00 model in a calm water test.

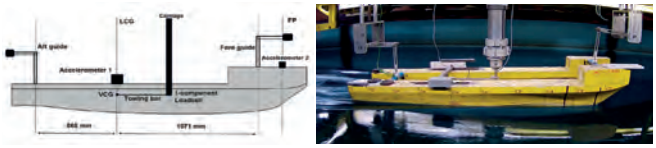

Fig 3. Model setup and measuring equipment

Validation of the numerical results was carried out at a speed of 3.78 m/s in calm water and waves, and the results are compared to the EFD results in Tables 3 and 4, respectively.

Tab. 3. CFD and EFD results in calm water at a speed of 3.78 m/s

R_T (N)		Trim angle (deg)		Rise-up (mm)	
CFD	EFD	CFD	EFD	CFD	EFD
32.18	32.40	2.5	2.5	6.6	6.8

Tab. 4. CFD and EFD results under three regular head waves

V (m/s)	Wave num.	(m)	T (sec)	$\lambda/_{Lpp}$	Acceleration amplitude at CG (m/s2)		Pitch amplitude (deg)	
					CFD	EFD	CFD	EFD
3.78	01	4.18	1.16	1.00	0.4	1.0	0.2	0.3
	02	6.26	1.42	1.50	4.6	4.7	2.2	1.7
	03	8.34	1.63	2.00	7.2	8.0	4.0	3.3

In the case of calm water, the results of the numerical simulation for resistance, dynamic trim, and rise-up show good agreement with the EFD results. However, under waves, the simulation results show considerable discrepancies from the EFD results. The highest deviation is seen for wave #01, where the motion is very small: the relative error is considerable, although the absolute error is not high. The CFD setup was regarded as verified, and was employed for further analysis.

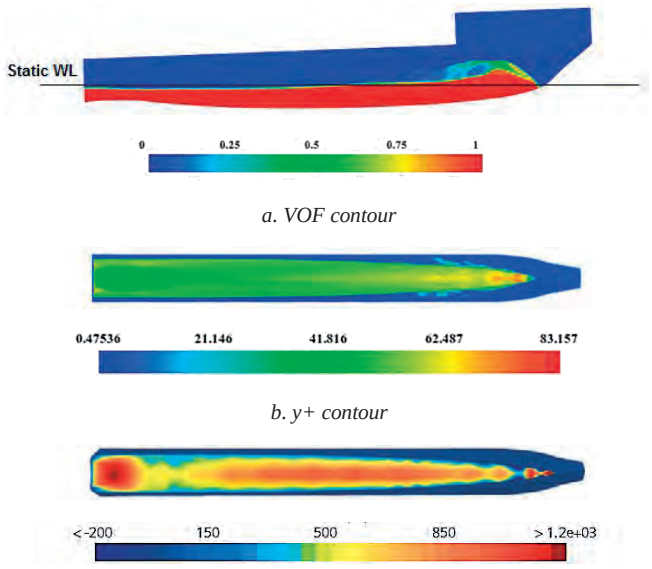

a. VOF contour

b. y+ contour

c. Pressure contour

Fig. 4. Detailed features of the AUT-SEM00 model in calm water at a speed of 3.78 m/s

Fig. 5(a) shows the wetted surface contour. It can be seen that the changes in the trim and draught are not high compared to the static condition. Fig. 5(b) shows the *y*+ contour on the wetted surface, which is within the range 30–100, defined as the optimal range in the ITTC recommendations of 2014 [18]. Fig. 5(c) shows the relative pressure, and it can be seen that the maximum pressure is located where the water touches the body at the fore and in an area around the stern, where the wetted surface ends. This kind of pressure distribution indicates that the dynamic trim is not likely to be much different from the initial static trim.

NUMERICAL SIMULATIONS OF A HIGH ASPECT RATIO SEMI-PLANING CATAMARAN

The aspect ratio is a parameter that can change a boat's hydrodynamic performance, and is defined as the ratio of the boat length to the demi-hull beam ($\Lambda = L/b$). In this section, we evaluate the hydrodynamic performance of an SPC in calm water and waves under extreme changes in its aspect ratio, using numerical simulations carried out in Star CCM+. For this purpose, we develop two new SPC hulls, denoted as AUT-SEM01 and AUT-SEM02, with aspect ratios of 19.18 and 29.61, respectively. These two new hulls with high aspect ratio are generated based on the geometry of AUT-SEM00, where the following constraints are met:

- The volume displacement of the generated hulls is equal to AUT-SEM00's displacement, to ensure a fair performance comparison.
- The ratio of the draught to beam of hull sections for the two generated hulls is the same as for AUT-SEM00.

SPECIFICATIONS OF THE THREE SPCS

Table 5 gives the main particulars of the three hulls at the model size, and Fig. 6 shows their relative sizes from a perspective view.

Tab. 5. Main particulars of three model SPCs with conventional, medium and high aspect ratio

Model	L_{OA} (m)	b (m)	Λ (-)	T at L_{CF} (m)	B on WL (m)	Δ (kg)
AUT-SEM00	2.250	0.215	10.48	0.107	0.627	34.12
AUT-SEM01	3.375	0.176	19.18	0.087	0.512	34.12
AUT-SEM02	4.500	0.152	29.61	0.076	0.443	34.12

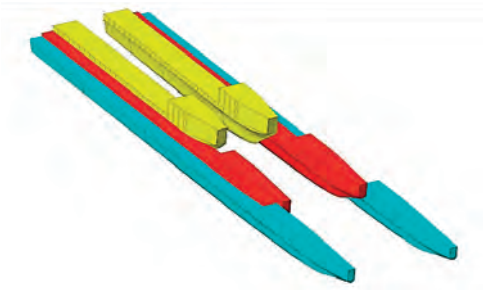

Fig 5. Perspective view of AUT-SEM00 (yellow), AUT-SEM01 (red) and AUT-SEM02 (green)

NUMERICAL SIMULATION RESULTS AND ANALYSIS

Numerical simulation scenario

Calm water model tests were performed at a speed of 3.78 m/s (equivalent to 30 knots for the ship) under static trim of 2.0°. Model tests were also performed under waves #01, #02 and #03, (i.e. regular head waves) at the same speed and static trim angle. ITTC has issued several recommendations for the model tests of ships in waves, as follows [19]:

- The wavelength should be in the range 0.50–2.00 LPP.
- The ratio of the wave height to wavelength must remain constant at about 1/50.

Performance in calm water

Having validated and verified our numerical simulation setup as described in Section 3.4, the same setup was used for AUT-SEM01 and AUT-SEM02. Fig. 6 shows the VOF, y^{+}, and pressure contours for AUT-SEM01 and AUT-SEM02.

In Figs. 6(a) and (d), it can be seen that the changes in the trim and draught are not high, indicating that the wetted surface is not very different from the static mode. Figs. 6(b) and (e) show that y+ is within the range recommended by the ITTC [19]. However, for the pressure on AUT-SEM01 and AUTSEM02, we see from Figs. 6(c) and (f) that there is a significant change in comparison with AUT-SEM00 in Fig. 4(c). This indicates that by increasing the aspect ratio, the pressure decreases, which can explain why the rise-up in the case of AUT-SEM00 becomes sinkage for AUT-SEM02. The same kind of pressure distributions are observed in comparison to AUT-SEM00, resulting in a dynamic trim that is close to the initial static trim.

Table 8 gives some quantitative results for the performance of the three models in calm water.

Tab. 6. Hydrodynamic performance results in calm water for three models with different aspect ratios

V(m/s)	Model	Λ (-)	R_T (N)	θ_D (Deg)	Z_v (mm)
3.78	AUT-SEM00	10.5	31.94	2.41	7.0
	AUT-SEM01	19.2	30.52	2.50	−0.1
	AUT-SEM02	29.6	31.32	2.49	−13.6

Table 8 indicates that the effect of the aspect ratio on the dynamic trim and the total resistance is insignificant, although it has a considerable effect on the rise-up: increasing the aspect ratio converts the rise-up to a considerable sinkage. To enable us to analyse the details of the resistance components of each model, Table 9 shows how the wetted surface and the resistance coefficients vary between the models. It can be seen that although the total resistance does not change substantially, the changes in the residual and frictional resistances are considerable: increasing the aspect ratio increases the frictional resistance and decreases the residual resistance. This is because increasing the aspect ratio increases the wetted surface, and decreases the residual resistance coefficient (CR) and friction resistance coefficient (CF), as shown in Table 12.

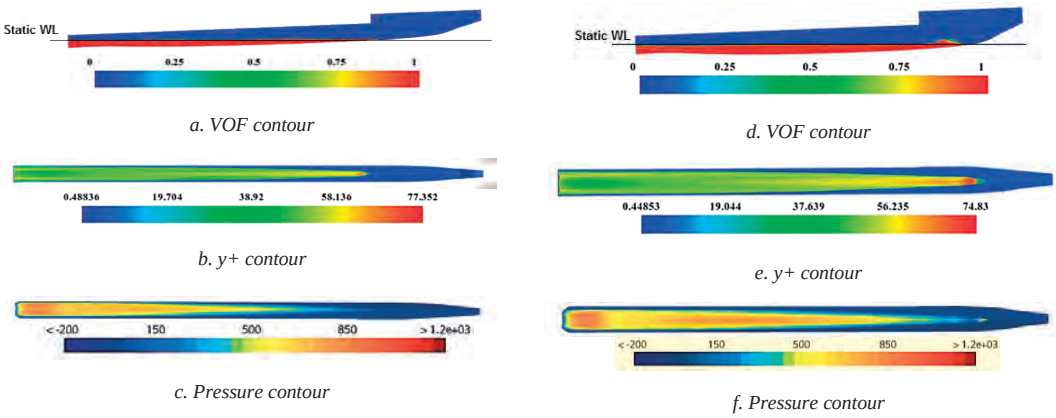

a. VOF contour

b. y+ contour

c. Pressure contour

d. VOF contour

e. y+ contour

f. Pressure contour

Fig 6. Results for the (a-c) AUT-SEM01 and (d-f) AUT-SEM02 models in calm water at a speed of 3.78 m/s

Tab. 7. Residual and frictional resistance

Model	Sw (m²)	C_T	C_F	C_R	R_T (N)	R_F (N)	R_R (N)
AUT-SEM00	1.07	0.004170	0.001298	0.002872	31.94	22.00	9.94
AUT-SEM01	1.15	0.003707	0.00096	0.002750	30.52	22.64	7.88
AUT-SEM02	1.22	0.003586	0.00095	0.002636	31.32	23.02	8.30

Fig. 7 shows the wetted surface, while Fig. 8 shows the C_T, $C_{R,}$ and C_F as functions of the aspect ratio. Fig. 9 shows the total, residual, and frictional resistance coefficients versus the aspect ratio.

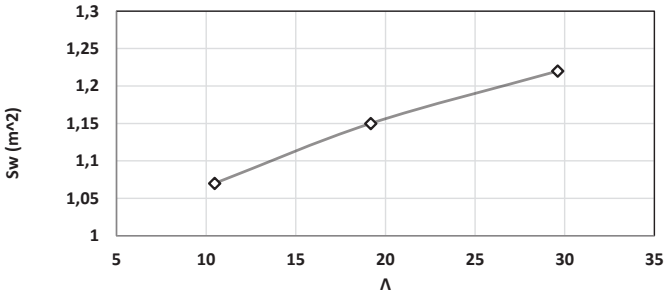

Fig. 7. Wetted surface versus aspect ratio

From Fig. 7, we see that for a given displacement, the wetted surface rapidly increases as the aspect ratio increases, which is due to the significant increase in model length.

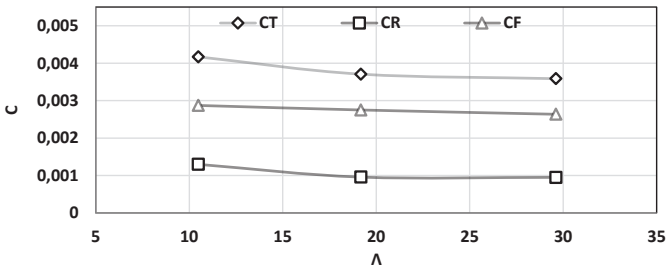

Fig 8. CT, CR, CF versus aspect ratio

Fig. 8 shows that increasing the aspect ratio causes a decrease in CT, which is strongly associated with a decrease in CR. This is because the model becomes more elongated with an increase in the aspect ratio.

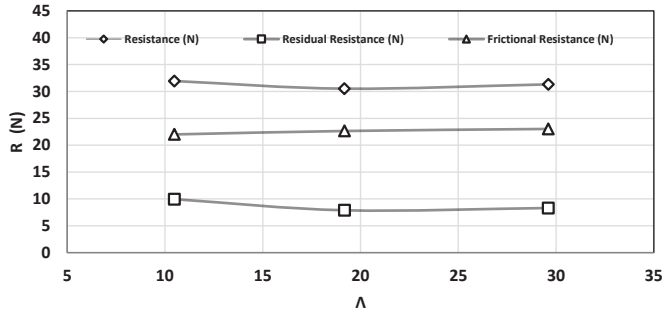

Fig. 9. Total, residual, and frictional resistances versus aspect ratio

As shown in Fig. 8, the frictional resistance and total resistance coefficients decrease as the aspect ratio increases. As can be seen in Fig. 9, the overall frictional resistance and total resistance are almost constant, due to the increase in the wetted surface (see the Fig. 7) as the aspect ratio increases.

Performance in regular waves

Numerical simulations on the three models were also conducted to capture their relative performance in regular waves. The motion and acceleration of each boat were evaluated at the model scale under waves, as described in Table 5, at a speed of 3.78 m/s in head sea conditions. Table 10 presents some quantitative results for the performance of each model, and Figs. 10–12 demonstrate how the performance varies with the aspect ratio. The performance change given in Table 10 is calculated using Eq. (10):

$$\left|\frac{X_{AUTSEM0i} - X_{AUTSEM00}}{X_{AUTSEM00}}\right| \times 100 \qquad (10)$$

Tab. 8. Aspect-ratio-induced percentage change in performances under waves at V= 3.78 m/s

Model	Wave	$\eta_{CG\ ACC}$ (m/s^2)	$\eta_{CG\ ACC}$ change (%)	η_θ (deg)	η_θ change (%)	η_3 (mm)	η_3 change (%)
AUT-SEM00	01	0.54	-	0.24	-	1.8	-
	02	4.83	-	2.22	-	32.3	-
	03	7.04	-	3.94	-	81.9	-
AUT-SEM01	01	0.18	–66.67	0.06	–75.00	0.6	–68.13
	02	3.33	–31.06	1.65	–25.68	21.7	–32.75
	03	6.26	–11.08	3.59	–8.88	66.5	–18.73
AUT-SEM02	01	0.08	–85.19	0.01	–95.83	0.7	–63.19
	02	0.85	–82.40	0.80	–63.96	4.6	–85.75
	03	4.81	–31.68	2.39	–39.34	51.0	–37.77

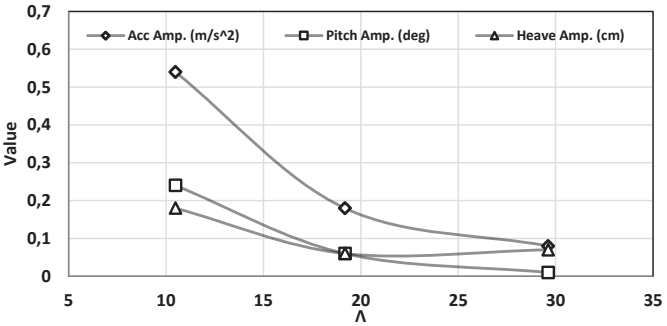

Fig 10. Effect of aspect ratio on the performance of each model under wave #01

In general, the aspect ratio has a strong impact on the performance of each model in waves. Increasing the aspect ratio significantly reduces the amplitudes of the heave and pitch, and in particular, the acceleration dramatically reduces as the aspect ratio increases.

Fig. 10 shows that the heave, pitch, and vertical acceleration under wave #01 generally decrease as the aspect ratio increases. However, at an aspect ratio of 29.6, a slight deviation from the general trend is observed. The pitch angle at this point is very small, with a value of about 0.07°, and its deviation from the general trend may be associated with the accuracy of the simulation.

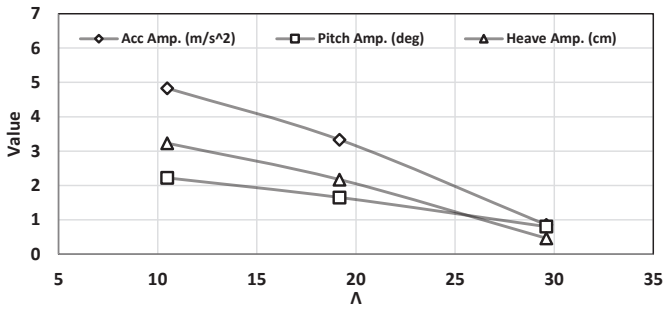

Fig. 11. Effect of aspect ratio on the performance of each model under wave #02

Fig. 11 also shows that the heave, pitch, and vertical acceleration under wave #02 undergo a decreasing trend that is more pronounced compared to wave #01.

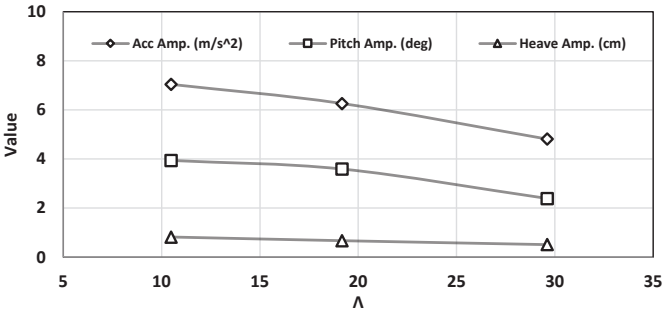

Fig. 12. Effect of aspect ratio on the performance of each model under wave #03

Furthermore, Fig. 12 shows that the heave, pitch, and vertical acceleration under wave #03 undergo a decreasing trend, with the heave amplitude showing a small slope, as the aspect ratio increases.

The main applications for these vessels are as crew-boats, passenger carriers, and so on. The degradation in their performance is mostly related to the high values of acceleration in sea waves. Table 13 and Figs. 14–16 show that AUT-SEM02 undergoes much less acceleration than the conventional catamaran, AUT-SEM00.

COMFORT ASSESSMENT SPECIFICATIONS

In this paper, we adopt the basic evaluation method given in ISO2631-1(1997), which is calculated according to Eq. (11) [20]:

$$\mathrm{RMS}=\left[\frac{1}{\bar{T}}\int_0^{\bar{T}} a_w{}^2(t)\,dt\right]^{\frac{1}{2}} \quad (11)$$

The vibration limits used in ISO2631-1(1997) include perception limits and comfort label as follows [20]:

1. Perception limit: 50% of alert and robust people have a detection limit of 0.015 m/s^2 (peak).
2. Comfort label: These are shown in Table 11.

Tab. 9. Comfort label in under vibration

RMS	Label
Less than 0.315 m/s	Not uncomfortable
0.315 m/s to 0.63 m/s	A little uncomfortable
0.5 m/s to 1 m/s	Fairly uncomfortable
0.8 m/s to 1.6 m/s	Uncomfortable
1.25 m/s to 2.5 m/s	Very uncomfortable
Greater than 2 m/s	Extremely uncomfortable

The RMS value of the acceleration at the CG is shown in Table 12 for different AUT-SEM models.

Tab. 10. Comfort label analysis for different AUT-SEM models

Model	Wave	RMS (m/s^2)	Label
AUT-SEM00	01	0.39	A little uncomfortable
	02	3.32	Extremely uncomfortable
	03	5.34	Extremely uncomfortable
AUT-SEM01	01	0.12	Comfortable
	02	2.14	Very uncomfortable
	03	4.57	Extremely uncomfortable
AUT-SEM02	01	0.07	Comfortable
	02	0.55	A little uncomfortable
	03	3.58	Extremely uncomfortable

Table 12 shows that with an increase in the aspect ratio from the AUT-SEM00 model to the AUT-SEM03 model, the level of comfort improves significantly: for wave #01, it changes from a little uncomfortable to not uncomfortable, and for wave #02, it changes from extremely uncomfortable to a little uncomfortable, thus giving a significant improvement in the comfort of the crew and passengers.

CONCLUSION

In this study, model tests and numerical simulations have been conducted on SPCs to investigate the effect of the aspect ratio. The following conclusions can be drawn:

- For a given displacement, as the aspect ratio increases, the wetted surface rapidly increases. However, increasing the aspect ratio causes a decrease in CT, which is mainly associated with a decrease in CR. These two contradictory effects cause the total resistance to be almost unchanged as the aspect ratio increases.
- The effect of the aspect ratio on the dynamic trim in calm water is insignificant, whereas it has a considerable effect on the rise-up. Increasing the aspect ratio may convert the rise-up to considerable sinkage.

- The heave, pitch, and vertical acceleration in waves generally decrease as the aspect ratio increases.
- For the case studied here, the vertical acceleration is reduced by up to 85% as the aspect ratio increases. Consequently, the seakeeping performance radically improves and the risk to crew and equipment is reduced.

NOMENCLATURE

Fr	Froude number
V	Speed in m/s
V_k	Speed in knots
u_τ	Frictional velocity
G	Gravitational acceleration
μ	Viscosity
$\overline{u_i}$, $\overline{u_j}$	Time-averaged velocity
L_{WL}	Waterline length
λ_w	Wane length
LOA	Overall length
B_T	Maximum transom beam
b	Demi-hull breadth
T	Draft
Δ	Displacement
ρ	Water density
λ	Scale factor
L_{CG}	Longitudinal centre of gravity
L_{CF}	Longitudinal centre of flotation
p	Apparent order of the GCI method
r	Grid refinement factor
E	Difference in model resistance for different grid sizes
ϕ_i	Solution (here R_T) on the i-th mesh
ea^{21}	Approximate relative error
e_{ext}^{21}	Aonvergence coefficient for the GCI network
T_F	Bow draft
T_A	Stern draft
θ_s	Static trim angle
Λ	Aspect ratio
l	Tank length
b	Tank width
H	Tank height
h	Tank depth
V_c	Carriage speed
$or\ L_{PP} L_{BP}$	Length between perpendiculars
T_W	Wave period
H_W	Wave height
C_T	Total resistance coefficient
C_F	Frictional resistance coefficient
C_R	Residual resistance coefficient
R_T	Total resistance
R_F	Frictional resistance
R_R	Residual resistance
θ_D	Dynamic trim
Z_v	Rise-up
S_w	Wetted surface
η_θ	Pitch motion amplitude
η_3	Heave motion amplitude
Y	Absolute distance from the wall
ϑ	Kinematic velocity
$\eta_{CG\ ACC}$	Amplitude of CG acceleration
$\overline{T}$	Duration
$a_w(t)$	Acceleration in m/s^2
RANS	Reynolds-averaged Navier–Stokes
CFD	Computational fluid dynamics
EFD	Experimental fluid dynamics
RAO	Response amplitude operator
RMS	Root mean square

REFERENCES

1. Millward A.The effect of hull separation and restricted water depth on catamaran resistance. Trans. R. Inst. Nav. Archit. 134, 341-349, 1992.

2. Zaraphonitis G, Spanos D, Papanikolaou A. Numerical and experimental study on the wave resistance of fast displacement asymmetric catamarans. Proc. 2nd Int. Euro Conference HIPER, vol. 1, 2001.

3. Moraes H B, Vasconcellos J M, Latite RG. Wave resistance for high-speed catamarans. Ocean Eng. 31(17-18), 2253-2282, 2004. doi:10.1016/j.oceaneng 2004.03.012.

4. Lee S H, Lee Y G, Kin S H. On the development of a small catamaran boat. Ocean Eng. 34(14-15), 2061-2073, 2007. doi:10.1016/j.oceaneng.

5. Zaghi S, Broglia R, Di Mascio A. Experimental and numerical investigations on fast catamarans interference effects. J. Hydrodyn. 22(5), 545-549, 2010. doi:10.1016/S1001-6058(09)60250-X.

6. Zaghi S, Broglia R, Di Mascio A. Analysis of the interference effects for high-speed catamarans by model tests and numerical simulations. Ocean Eng. 38(17-18), 2110-2122, 2011. doi:10.1016/j.oceaneng 2011.09.037.

7. Farkas A, Degiuli N, Martić I. Numerical investigation into the interaction of resistance components for a series 60 catamaran. Ocean Eng. 146(August), 151-169, 2017. doi:10.1016/j.oceaneng 2017.09.043.

8. Lin C T, Lin T, Lin C W, Hsieh Y W, Lu L, Hsin C Y. Investigation of the seakeeping performance of twin hull vessels by different computational methods. 10th International Workshop on Ship and Marine Hydrodynamics Keelung. Taiwan, November 5th-8th, 2017.

9. Fitriadhy A, Adam N, Amalina N, Azmi S.A. Seakeeping prediction of deep-V high-speed catamaran using

computational fluid dynamics approach. SINERGI 22(3), 139-148, 2018. doi:10.22441/sinergi.2018.3.001.

10. Chen X, Zhu R., Chuan Song Y, Lan, Fan J. An investigation on HOBEM in evaluating ship wave of high-speed catamaran ship. J. Hydrodyn. 31(3), 531-541, 2019. doi:10.1007/s42241-018-0092-8.

11. Honaryar A, Ghiasi M, Liu P, Honaryar A. A new phenomenon in interference effect on catamaran dynamic response. International Journal of Mechanical Sciences 190, 106041, 2021. doi:10.1016/j.ijmecsci.2020.106041.

12. Dogrul A, Kahramanoglu E, Cakıcı F. Numerical prediction of interference factor in motions and added resistance for Delft catamaran 372. Ocean Engineering 223, 108687, 2021. doi:10.1016/j.oceaneng.2021.108687.

13. Farkas A, Degiuli N, Tomljenović I, Martić I. Numerical investigation of interference effects for the Delft 372 catamaran. In: Sustainable development and innovations in marine technologies (pp. 67-74). CRC Press. 2022. doi:10.1177/14750902231197886.

14. Windyandari A, Sugeng S, Sulaiman, Ridwan M, Kurniawan Yusim A. Seakeeping behavior of hexagonal catamaran hull form as an alternative geometry design of flat-side hull vessel. Journal of Applied Engineering Science 21(4), 1016-1030, 2023. doi:10.5937/jaes0-41412.

15. Moghaddas A, Zeraatgar H. Investigation of the static trim angle effects on the hydrodynamic performances of a semi-planing catamaran in calm water and waves. Scientia Iranica (under publication).

16. ITTC Recommended Procedures and Guidelines. Practical guidelines for ship CFD application. 7.5-03-02-03. Revision 01. 2011.

17. Celik I, Ghia U, Roache P, Freitas C, Coleman H, Raad P. Procedure for estimation and reporting of uncertainty due to discretization in CFD applications. J. Fluids Eng. 130(7), 078001-078004, 2008. DOI:10.1115/1.2960953.

18. ITTC Recommended Procedures and Guidelines. Practical guidelines for ship CFD application. 7.5-03-02-03. Revision 01. 2011.

19. ITTC Recommended Procedures and Guidelines. Seakeeping Experiments. 7.5-02 -07-02.1. Revision 04. 2014.

20. ISO 2631. Mechanical vibration and shock-evaluation of human exposure to whole-body vibration. Part 1: General Requirements. International Organization for Standardization, Geneva, Switzerland, 1997.